Supporting Information

Quantum Mechanical/Molecular Mechanical Study of the HDV Ribozyme: Impact of the Catalytic Metal Ion on the Mechanism

Abir Ganguly, Philip C. Bevilacqua,* and Sharon Hammes-Schiffer*

Department of Chemistry, 104 Chemistry Building, The Pennsylvania State University, University Park, Pennsylvania 16802

*Corresponding authors: pcb@chem.psu.edu, shs@chem.psu.edu

Molecular Dynamics (MD) equilibration procedure

The equilibration procedure for the starting structure of the QM/MM calculations was as follows:

1. Energy optimization of the solvent (waters, Na^+ and Cl^- ions) with the solute (RNA and crystallographic Mg^{2+}) fixed.

2. Simulated annealing (NVT ensemble, Nosé-Hoover thermostat[1,2]) of solvent keeping solute fixed:

i. Increase temperature from 0K to 298K in 10 ps, MD @ 298 K for 50 ps

ii. Increase temperature from 298K to 498K in 10 ps, MD @ 498K for 50 ps

iii. Increase temperature from 498K to 698K in 10 ps, MD @ 698K for 50 ps

iv. Decrease temperature from 698K to 498K in 10 ps, MD @ 498K for 50 ps

v. Decrease temperature from 498K to 298K in 10 ps, MD @ 298 K for 150 ps

The above protocol was performed two times.

3. MD at 298K with NPT ensemble using Nosé-Hoover barostat[1,2] for 100 ps with solute fixed.

Supporting References:

(1) Nosé, S. *Mol. Phys.* 1984, 52, 255-268.
(2) Hoover, W. G. *Phys. Rev. A* 1985, 31, 1695-1697.

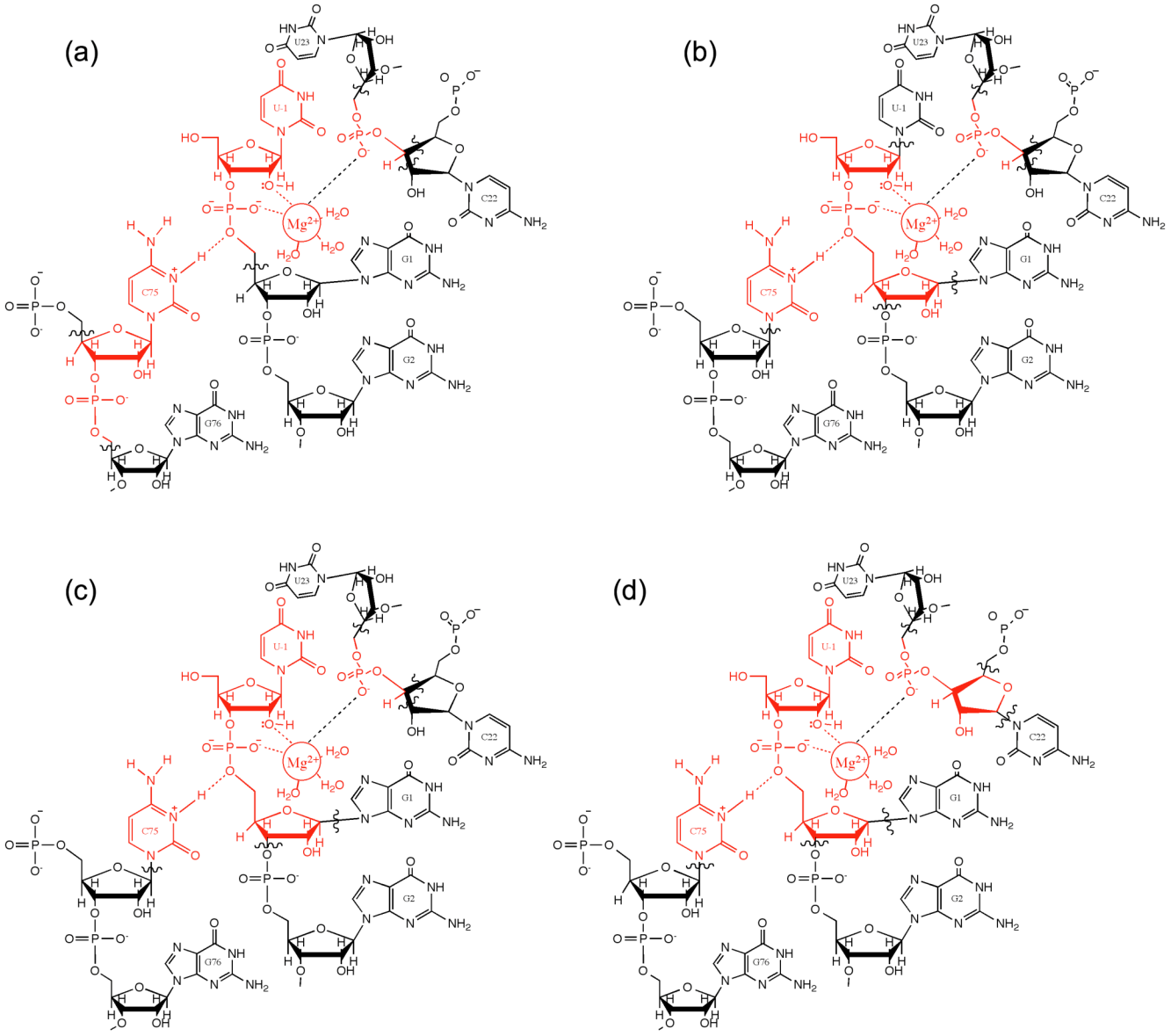

Figure S1. QM regions considered for the QM/MM calculations. Atoms in red are included in the QM region. Wavy lines indicate the QM-MM boundary. Table S1 provides the key distances after a QM/MM optimization with each of these QM regions. Region (d), which contains 87 QM atoms, was chosen for the subsequent calculations used to generate the results in the paper and is depicted in Figure 1.

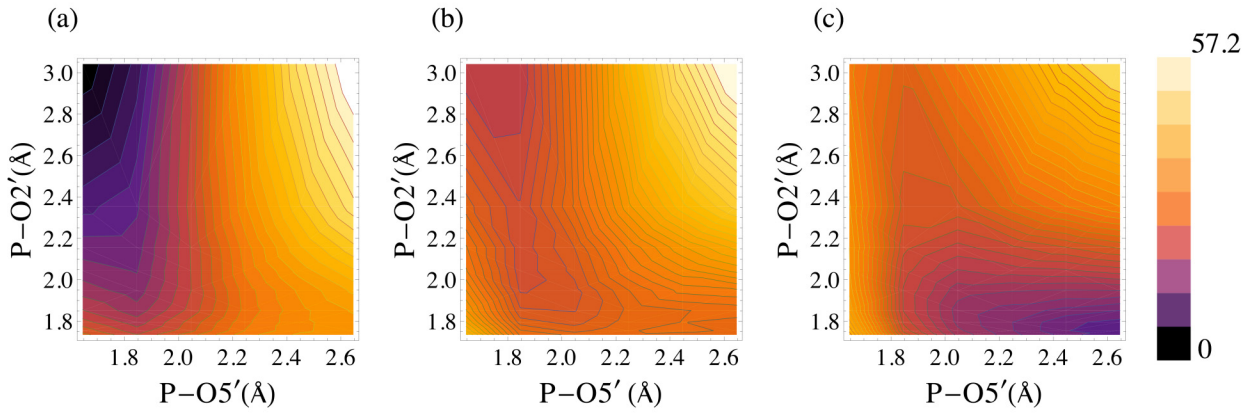

Figure S2. Potential energy surfaces obtained from constrained optimizations along P(G1)-O5′(G1) and P(G1)-O2′(U-1) coordinates for (a) H3 bonded to N3 of C75, (b) H3 in the middle of N3(C75) and O5′(G1) at the TS position, (c) H3 bonded to O5′(G1). The legend for the color-coding is shown on the extreme right in units of kcal/mol. In part (a), to mimic the proton transfer reactant state, the H3(C75)-N3(C75) distance was constrained to its value in the optimized reactant structure. In part (b), to mimic the proton transfer transition state, the H3(C75)-N3(C75), H3(C75)-O5′(G1), and N3(C75)-O5′(G1) distances were constrained to the distances in the TS. In part (c), to mimic the proton transfer product state, the H3(C75)-O5′(G1) distance was constrained to its value in the optimized product structure. To generate each point on the potential energy surfaces, the P-O5′ and P-O2′ interatomic distances, as well as the relevant proton transfer interface distances, were constrained while all other coordinates were optimized using the QM/MM methods described in the paper. The minimum observed in panel (a) (top left of the surface) corresponds to the reactant state, and the minimum observed in panel (c) (bottom right of the surface) corresponds to the product state. No minima corresponding to intermediate states were observed.

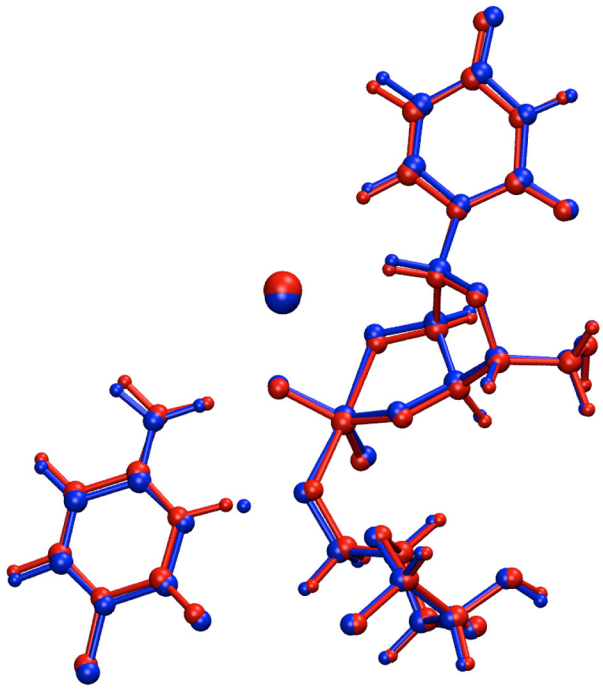

Figure S3. Overlay of the phosphorane-like transition state (blue) obtained with bound Mg^{2+} with the phosphorane intermediate (red) obtained with bound Na^{+}. The main difference is in the position of the H3 proton, which is midway between N3(C75) and O5′(G1) in the transition state but bonded to N3(C75) in the phosphorane intermediate. C75 is shown in the lower left of the figure.

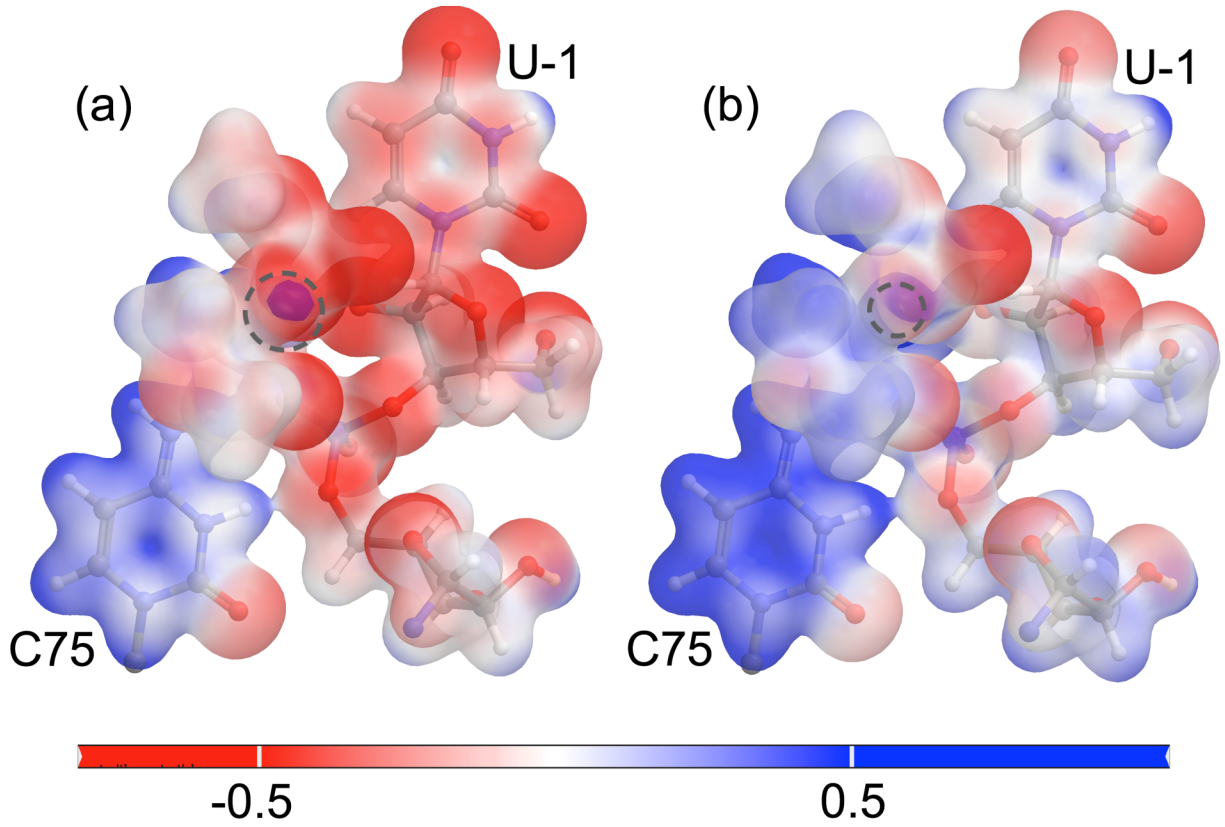

Figure S4. Molecular electrostatic potential mapped onto the electron density isosurface. The QM region is shown here for the (a) optimized reactant state with the Mg^{2+} at the catalytic position, with the Mg^{2+} ion replaced by a Na^{+}, and (b) optimized reactant state with a Na^{+} ion at the catalytic position, with the Na^{+} ion replaced by a Mg^{2+}. In both panels, the scale is from -0.5 to 0.5 kT/e at 298 K. The dotted gray circle indicates the position of the metal ion in each case. The similarity of panel (a) with Figure 4(b) and of panel (b) with Figure 4(a) suggests that the difference in the electrostatic potential of the residue C75 is governed by the presence of a divalent or a monovalent ion at the catalytic site, rather than structural differences.

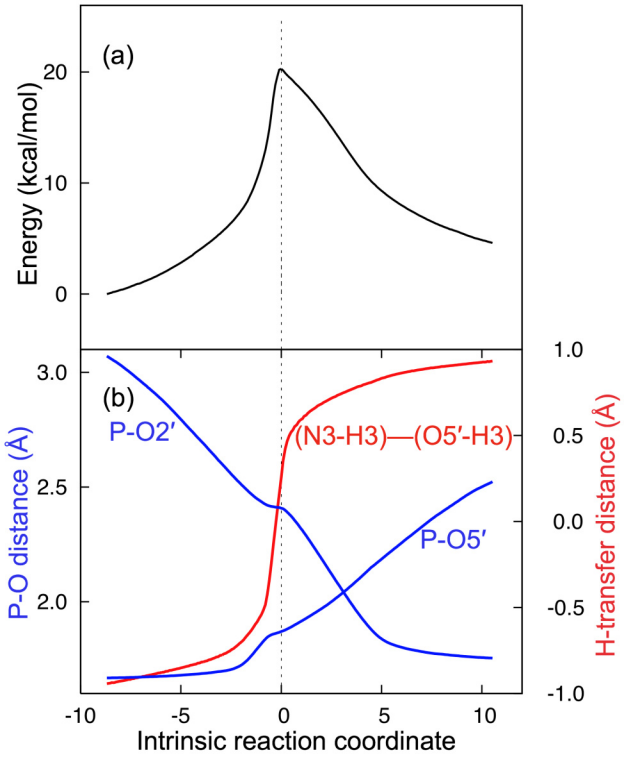

Figure S5. Minimum energy path (MEP) for the self-cleavage reaction obtained using QM/MM methods with Ca^{2+} at the catalytic site. The energy (a) and relevant distances (b) are shown along the intrinsic reaction coordinate.

	crystal structure	Region (a)	Region (b)	Region (c)	Region (d)
N3(C75)-O5′(G1) (Å)	3.58	3.51	3.24	3.25	3.22
N3(C75)-H-O5′(G1) (˚)	154.43	162.75	163.25	160.93	157.0
Mg^{2+}-HOH (1) (Å)	1.97	2.20	2.26	2.19	2.19
Mg^{2+}-HOH (2) (Å)	1.98	2.04	2.05	2.04	2.05
Mg^{2+}-HOH (3) (Å)	1.91	2.13	2.14	2.13	2.13
Mg^{2+}-O2′(U-1) (Å)	2.37	2.30	2.29	2.28	2.28
Mg^{2+}-O1P(U23) (Å)	2.24	1.94	1.93	1.94	1.95
O2′(U-1)-P(G1) (Å)	3.30	3.12	3.10	3.08	3.09
N4(C75)-O2P(G1) (Å)	3.58	3.41	3.13	3.16	3.14

Table S1. Comparison of key distances and angles in the active site of the HDV ribozyme after QM/MM optimization with the QM regions depicted in Figure S1. Based on these values, region (d) was chosen for the subsequent calculations used to generate the results in the paper. Region (a) was eliminated because the H-cap on C5′(G1) was too close to the reaction center and affected the N3(C75)-O5′(G1) distance. Region (b) was eliminated because the exclusion of the U-1 residue affected the Mg^{2+}-HOH (1) distance. Region (c) was eliminated because H-capping inside the C22 sugar led to artifacts in frequency calculations. Note that the optimized reactant structure for region (d) differs slightly from that reported in the paper because the optimization of the reactant reported in this table was performed directly from the starting structure, while the optimized reactant reported in the paper was obtained from the minimum energy path starting at the transition state.

	TS with Mg^{2+}	TS with Ca^{2+}	PI with Li^{+}	PI with Na^{+}	PI with K^{+}
N3(C75)-O5′(G1) (Å)	2.63	2.64	2.94	2.91	2.89
N3(C75)-H3(C75) (Å)	1.32	1.45	1.05	1.06	1.06
O5′(G1)-H3(C75) (Å)	1.31	1.19	1.90	1.86	1.84
P(G1)-O5′(G1) (Å)	2.05	1.87	1.81	1.85	1.86
P(G1)-O2′(U-1) (Å)	1.95	2.41	1.95	1.91	1.89
P(G1)-O2P(G1) (Å)	1.56	1.53	1.57	1.56	1.56
O1P(G1)-O2P(G1)-P(G1)-O3′(U-1) (improper dihedral) (°)	178.6	160.4	175.2	179.5	178.9

Table S2. Comparison of the active site distances and angle of the phosphorane-like transition state (TS) with a Mg^{2+} or Ca^{2+} ion at the catalytic position and the phosphorane intermediate (PI) with monovalent ions at the catalytic position.

	Mg^{2+}	Ca^{2+}	Li^{+}	Na^{+}	K^{+}
Reactant	0	0	0	0	0
TS/PI	25.1	20.3	3.7	6.5	9.0
Product	10.3	4.6	–12.7	–16.0	–14.7

Table S3. Comparison of the QM/MM energies of the solvated ribozyme system with different ions at the catalytic position. The energies are expressed in units of kcal/mol, relative to the respective reactant states. The energies in the second row correspond to the phosphorane-like transition state (TS) for Mg^{2+} and Ca^{2+} (red) and to the phosphorane intermediate (PI) for Li^{+}, Na^{+} and K^{+} (blue).